

# Chaos in Charged Gauss-Bonnet AdS Black Holes in Extended Phase Space

Sandip Mahish<sup>1</sup> and Chandrasekhar Bhamidipati<sup>2</sup>

School of Basic Sciences  
Indian Institute of Technology Bhubaneswar  
Jatni, Khurda, Odisha, 752050, India

## Abstract

We study the onset of chaos due to temporal and spatially periodic perturbations in charged Gauss-Bonnet AdS black holes in extended thermodynamic phase space, by analyzing the zeros of the appropriate Melnikov functions. Temporal perturbations coming from a thermal quench in the unstable spinodal region of P-V diagram, may lead to chaos, when a certain perturbation parameter  $\gamma$  saturates a critical value, involving the Gauss-Bonnet coupling  $\alpha$  and the black hole charge  $Q$ . A general condition following from the equation of state is found, which can rule out the existence of chaos in any black hole. Using this condition, we find that the presence of charge is necessary for chaos under temporal perturbations. In particular, chaos is absent in neutral Gauss-Bonnet and Lovelock black holes in general dimensions. Chaotic behavior continues to exist under spatial perturbations, irrespective of whether the black hole carries charge or not.

arXiv:1902.08932v3 [hep-th] 23 Jun 2019

---

<sup>1</sup> sm19@iitbbs.ac.in

<sup>2</sup> chandrasekhar@iitbbs.ac.in

# 1 Introduction

Black hole solutions and their thermodynamics in General Relativity have thrown up remarkable surprises and continue to be an intriguing area of research. In particular, phase transitions of black holes in a variety of backgrounds, such as Anti de Sitter (AdS) space-time have been actively pursued, purely from gravity point of view and also with holographic motivations in mind [1]-[9]. More recently, treating the cosmological constant as a dynamical thermodynamical variable (pressure), an extended phase thermodynamics has been proposed, where the first law of black hole mechanics gets modified by a new  $pdV$  term [10]-[21]. Study of PV critical behavior of various black holes confirms the existence of an exact map of black hole small/large phase transitions to the Van der Waals liquid/gas system [22]-[26].

It is known that chaos is unavoidable in certain dynamical systems in nature, including black hole physics and cosmology [27]-[34]. There have been several past works probing chaotic behavior in black holes by various methods, such as, computation of Lyapunov exponents to study stability of orbits, quasinormal modes in Reissner-Nordstrom and Gauss-Bonnet black holes [35, 36], and Melnikov's [37] method in the context of geodesic motion [27-29]. However, the study of chaos in the context of black hole thermodynamics and phase transitions has only just started emerging [38], partly due to the recent developments where a pressure term in the first law is included, making the connection with Van der Waals system exact[22]-[26]. In [38], the Melnikov method used in dynamical systems [37]-[41], developed in the context of Van der Waals system [43], was applied to the case of black holes in extended phase space to extract useful information about the presence of chaos. Temporal and spatial period perturbations were introduced in the PV thermodynamic phase space and the presence of chaos was detected from the study of zeros of Melnikov function. A bound involving charge of the black hole was also found, beyond which the system becomes chaotic.

In this letter, we take these issues forward by studying chaos in extended thermodynamic phase of black holes, after incorporating the effects of higher curvature terms in Einstein Action. We focus on the case of Gauss-Bonnet(GB) black holes, but the results are also spelled out for Lovelock black holes. Gauss-Bonnet and Lovelock terms are quite important in various contexts such as, semi-classical quantum gravity, low energy effective action of string theory and next to leading order large N corrections of boundary conformal field theory (CFT) studies in holography [47]-[66]. They are known to have given interesting insights in to the corrections to black hole entropy, viscosity to entropy ratio and several other recent developments in extended phase space [53, 55-58, 60]. Chaotic dynamics of test objects and instability of certain orbits, in particular, in the context of holography and Gauss-Bonnet theories has also been explored before [36, 67, 68], however, not from thermodynamic point of view. The extended phase thermodynamics of Gauss-Bonnet black holes in AdS (where the cosmological constant is taken to be dynamical) and its connection to the Van der Waals liquid/gas system via PV criticality is now well studied [61]. Following the study of chaotic behavior for Reissner-Nordstrom black holes in AdS, it is important to know whether the behavior found in [38] is a generic feature of systems exhibiting Van der Waals type phase transitions. With this motivation, we thus study chaotic dynamics in Gauss-Bonnet and other higher derivative theories of gravity, with the inclusion of an additional parameter, such as the Gauss-Bonnet coupling, in addition to charge

(considered in [38]), and find that there appears a new inequality which governs the existence of chaos. We also show that neutral Gauss-Bonnet black holes in five and higher dimensions, in contrast, do not show chaotic behavior under temporal perturbations, despite the fact that Van der Waals type phase transition and PV criticality exists [61]. We generalize this result to generic black holes systems which have an extended thermodynamic phase space description and starting from the equation of state, we find a new relation which can be used to rule out chaos. However, chaotic behavior under spatial perturbations in the unstable thermodynamic region, continues to exist for charged, as well as, neutral black holes. The results are also extended to Lovelock black holes in various dimensions.

Rest of the paper is organized as follows. In section-2, we recall the definition of Melnikov function and few known aspects of thermodynamics of GB black holes in extended phase space formalism. Section-3 deals with the effect of having a small temporal perturbation in the spinodal region of GB black hole thermodynamic phase space. We first obtain the analogue Hamiltonian system starting from the equation of state of the GB black hole, leading to the determination of homoclinic/heteroclinic orbits. Using the solutions for these orbits, the Melnikov function is computed explicitly and its zeros are analyzed, which give a bound on the parameter  $\gamma$  (following from a small temporal perturbation, to be introduced in section-3) for existence of chaotic behavior. This bound is also discussed for Lovelock black holes in higher dimensions and a general condition for ruling out chaos in any black hole is obtained. In section-4, the effect of a small spatial perturbation leading to the onset of chaos is discussed for GB black holes. Section-5 contains conclusions.

## 2 Melnikov's Method and Charged Black Holes in AdS

We start in subsection-(2.1) by summarising the basic technique due to Melnikov for studying the onset of chaotic behavior in Hamiltonian systems. In the following subsection-(2.2), we collect main results on charged Gauss-Bonnet black holes in AdS. These are then used for the computation of Melnikov function in sections-(3) and (4), for studying temporal and spatial perturbations, respectively in charged Gauss-Bonnet black holes.

### 2.1 Melnikov's Method for Perturbation of Hamiltonian Systems

To understand the Melnikov method, it is useful to start from an evolution equation for a displacement function  $x(t)$  as follows:

$$\dot{x} = f_0(x) + \epsilon f_1(x, t), \quad x \in \mathfrak{R}^{2n}, \quad (2.1)$$

with the following assumptions. First,  $\epsilon \ll 1$ , corresponding to a small perturbation and the function  $f_1(x, t)$ , is taken to be periodic in  $t$ . Second, the unperturbed system is Hamiltonian with smooth flow, conserving energy and contains a fixed point which is a homoclinic orbit<sup>1</sup>. There are further non-resonance assumptions on the function  $f_1(x, t)$ , which are necessary for smooth period perturbations and are given in the appropriate sections below. Figure-(1) shows sample plots of homoclinic and heteroclinic orbits. For homoclinic orbits, the stable  $W^s$  and

---

<sup>1</sup>The Melnikov method also works for heteroclinic orbits connecting two saddle points and irrespective of whether the solution  $x_0(t)$  is known analytically or not.

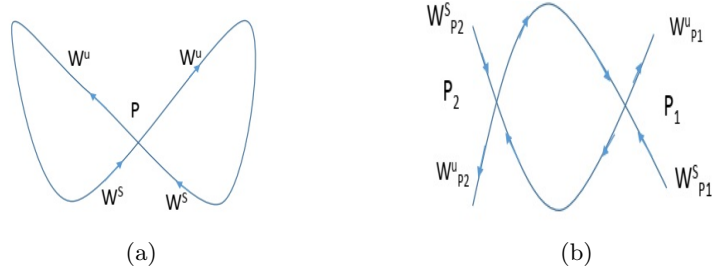


Figure 1: (a) Homoclinic orbit . (b) Heteroclinic orbit

unstable  $W^u$  manifolds of the saddle connect to each other at the hyperbolic fixed point  $P$ , while for heteroclinic orbits, the stable manifold of one saddle joins the unstable manifold of the other saddle, as seen in figure-(1). Now, under a temporal/spatial perturbation of the system,

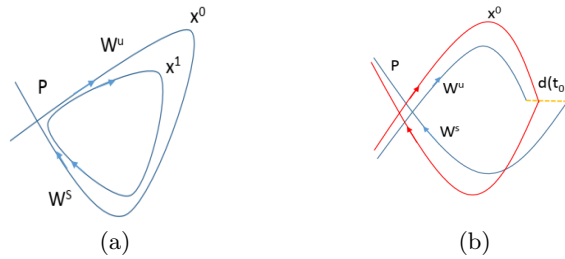


Figure 2: Homoclinic orbit: (a) Before perturbation. (b) After perturbation

there will be infinite number of complicated intersection points of stable and unstable manifolds (as it takes an infinite time to approach a saddle point). If the unperturbed homoclinic orbit is considered to be a curve parametrized by time, then at time  $t_0$ , the stable and unstable manifolds are separated by a perpendicular distance (as shown in figure-(2)) given as

$$d(t_0) = \frac{\epsilon M(t_0)}{|\mathbf{f}(x_0(0))|}.$$

Here,  $M(t_0)$  is known to be the the Melnikov function and its explicit form can be shown to be [37]-[41]:

$$M(t_0) = \int_{-\infty}^{+\infty} \mathbf{f}_0^T(x_0(t-t_0)) \Omega_n \mathbf{f}_1(x_0(t-t_0), t) dt, \quad (2.2)$$

with,

$$\Omega_{n=2} = \begin{pmatrix} 0 & 1 & 0 & 0 \\ -1 & 0 & 0 & 0 \\ 0 & 0 & 0 & 1 \\ 0 & 0 & -1 & 0 \end{pmatrix} \quad \text{and} \quad \Omega_{n=1} = \begin{pmatrix} 0 & 1 \\ -1 & 0 \end{pmatrix}. \quad (2.3)$$

Here, the subscript 1 and 2 stand for the number of degrees of freedom appearing in temporal and spatial perturbations, respectively. Melnikov function  $M(t_0)$ , is thus an estimate of the distance  $d(t_0)$  for the transverse intersections of stable and unstable orbits. If  $M(t_0)$  has a

simple zero as a function of  $t_0$ , then for  $\epsilon > 0$  and for suitably small value, the stable and unstable manifold of the Hamiltonian system intersect transversally [37]-[41]. From Smale-Birkhoff theorem [42], presence of such intersecting orbits implies that the Poincare Map has a invariant hyperbolic set: a Smale horseshoe, which is an indicator of chaos [41, 46].

## 2.2 Charged Gauss-Bonnet Black Holes in AdS

We start with some preliminaries on thermodynamics of black holes in extended phase space and defining the spinodal region where chaos is found. The Einstein-Maxwell action with a Gauss Bonnet term and a cosmological constant  $\Lambda$ , in  $d$  dimensions is as follows:

$$S = \frac{1}{16\pi} \int d^d x \sqrt{-g} [R - 2\Lambda + \alpha_{GB} (R_{\mu\nu\gamma\delta} R^{\mu\nu\gamma\delta} - 4R_{\mu\nu} R^{\mu\nu} + R^2) - 4\pi F_{\mu\nu} F^{\mu\nu}], \quad (2.4)$$

where  $\alpha_{GB}$  is Gauss Bonnet coupling and  $\Lambda = -\frac{(d-1)(d-2)}{2l^2}$ .  $F_{\mu\nu}$  is the Maxwell field strength, defined as  $F_{\mu\nu} = \partial_\mu A_\nu - \partial_\nu A_\mu$ , with the vector potential  $A_\mu$ . Here we will mostly consider the case with  $\alpha_{GB} \geq 0$ . The Gauss Bonnet term, proportional to  $\alpha_{GB}$  in the above action, is a topological term in four dimensions and hence we take  $d \geq 5$ . The solution for a static charged GB black hole is given as:

$$ds^2 = -f(r)dt^2 + \frac{dr^2}{f(r)} + r^2 d\Omega_{d-2}^2, \quad (2.5)$$

where  $d\Omega_{d-2}^2$  is a line element of  $(d-2)$  dimensional maximally symmetric Einstein space with volume  $\Sigma_k$  where  $k$  can be 1,0,-1, corresponding to spherical, Ricci flat and hyperbolic topology of black hole horizon, respectively. We will mainly deal with horizon of spherical topology. The general metric function is given by [61]

$$f(r) = k + \frac{r^2}{2\alpha} \left( 1 - \sqrt{1 + \frac{64\pi\alpha M}{(d-2)\Sigma_k r^{d-1}} - \frac{2\alpha Q^2}{(d-2)(d-3)r^{2d-4}} - \frac{64\pi\alpha P}{(d-1)(d-2)}} \right). \quad (2.6)$$

Here  $\alpha = (d-3)(d-4)\alpha_{GB}$ ;  $M$  and  $Q$  are mass and charge of black hole, and the pressure  $P = -\frac{\Lambda}{8\pi}$ . Notice that we have considered the cosmological constant to be a thermodynamic variable and replaced it with pressure as is the norm in extended thermodynamic phase space approach. The equation of state can be written as [61]:

$$P = \frac{d-2}{4r} \left( 1 + \frac{2k\alpha}{r^2} \right) T - \frac{(d-2)(d-3)k}{16\pi r^2} - \frac{(d-2)(d-5)k^2\alpha}{16\pi r^4} + \frac{Q^2}{8\pi r^{2d-4}}. \quad (2.7)$$

Thus, the first law in extended phase space is:

$$dM = TdS + \Phi dQ + VdP + \mathcal{A}d\alpha, \quad (2.8)$$

where  $S$  is the entropy,  $\Phi$  is the electric potential and  $\mathcal{A}$  is conjugate to the GB coupling  $\alpha$ . Hawking temperature  $T$  the thermodynamic volume  $V$  are given respectively as

$$T = \frac{1}{4\pi} f'(r) = \frac{16\pi P r^4 / 3 + 2kr^2 - \frac{2Q^2}{3r^2}}{4\pi r(r^2 + 2k\alpha)}, \quad (2.9)$$

and

$$V = \frac{\Sigma_k r_h^{d-1}}{d-1}. \quad (2.10)$$

Equation of state in five dimensions is thus:

$$P = \frac{T}{v} \left( 1 + \frac{32\alpha k}{9v^2} \right) - \frac{2k}{3\pi v^2} + \frac{512Q^2}{729\pi v^6}, \quad (2.11)$$

where the specific volume  $v = \frac{4r}{d-2} = \frac{4r}{3}$ . The Melnikov method is well suited for studying chaotic behavior in the black hole systems which follow Van der Waals equation for phase transition in the extended phase space formalism. To study the behavior of the system in spinodal region, the  $P-v$  phase diagram is introduced in figure-(3), where the labeling of different points is explained below. Denoting  $\delta P = \partial P(v, T_0)/\partial v$  and for a temperature  $T'$  below critical temperature, the

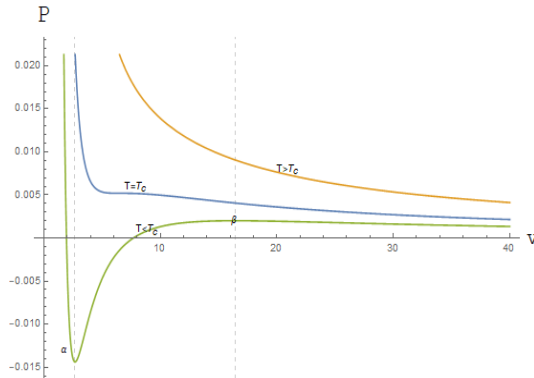


Figure 3: P-v diagram for the Gauss-Bonnet AdS Black hole

phase space of specific volume, i.e.,  $v \in [0, \infty]$ ), is divided into three regimes.  $[0, \alpha]$  corresponds to the region where small black holes exist, i.e., the fluid being in liquid phase, i.e.,  $\delta P < 0$ .  $[\alpha, \beta]$  corresponds to an unstable region, where small and large black hole phase co-exists, i.e.,  $\delta P > 0$ . The two points  $\alpha$  and  $\beta$  are determined by  $\delta P|_{v=\alpha} = \delta P|_{v=\beta} = 0$ . This is the main region of interest in the present case, called the spinodal domain, where a temporal or spatial periodic perturbation leads to chaos under certain conditions, to be discussed below.  $[\beta, \infty]$  corresponds to the large black hole domain, i.e., the fluid being vapor and where  $\delta P < 0$ .

### 3 Temporal Chaos in Spinodal region

Here, we study the effect of a small temporally periodic perturbation, when the system is quenched to the unstable spinodal region. We first compute the Hamiltonian for the fluid flow using the black hole equation of state and obtain the Melnikov function, which contains information about the onset of chaos. Let us start by considering a specific volume  $v_0$  corresponding to an isotherm  $T_0$ , which is fluctuated as follows [38, 43]:

$$T = T_0 + \epsilon \gamma \cos(\omega t) \cos(X) \quad \text{with} \quad \epsilon \ll 1. \quad (3.1)$$

The fluid flow is assumed to be taking place along the x-axis in a tube of unit cross section with fixed volume, which contains a total of mass  $2\pi/q$  of fluid in a volume  $(2\pi/q)v_0$ , where  $q > 0$  is a constant [43]. The fluid is further assumed to be thermoelastic, slightly viscous and isotropic with an additional stress following from the van der Waals-Korteweg theory of capillarity [43]. Here,  $X$  represents a column of black hole of unit cross section taken between certain points and

the details together with other assumptions are similar to earlier considerations given in [38, 43]. In present case the Hamiltonian is symbolically given to be [38, 43]:

$$H = \frac{1}{\pi} \int_0^{2\pi} \left[ \frac{u^2}{2} + \mathcal{F}(v, T) + \frac{Aq^2}{2} \left( \frac{\partial v}{\partial X} \right)^2 \right] dX \quad (3.2)$$

where  $u(x, t) = x_t(X, t)$  is the velocity of the reference fluid particle and  $A$  is a constant. Here,

$$\mathcal{F}(v, T) = - \int \bar{P}(v, T) dv, \quad (3.3)$$

with

$$\bar{P}(v, T) = P(v, T) \frac{dV}{dv} = \frac{4\pi Q^2}{9v^3} + \frac{9}{128} \pi^2 (-6kv + 9Tv^2 + 32kT\alpha). \quad (3.4)$$

$\bar{p}(v, T)$  is an effective equation of state obtained by replacing  $v$  in terms of the thermodynamic volume  $V = \frac{\pi v^3}{6}$  before performing the integral. Let us also note that the use of effective equation of state in eqn. (3.4) is important for existence or non-existence of chaos below. This is important as the Gibbs free energy written in terms of thermodynamic volume remains unchanged during phase transition and it is the combination  $PdV$  that has the right scaling [62, 63]. Following the approach in [38, 43], ignoring coefficients of order  $\mathcal{O}(1/v^4)$  in Taylor series expansion, the Hamiltonian can be computed to be:

$$\begin{aligned} H(x, u) &= \frac{u_1^2 + u_2^2}{2} - \frac{\bar{P}_v}{2}(v_0, T_0)(x_1^2 + x_2^2) - \frac{\bar{P}_{v,v}}{4}(v_0, T_0)x_1^2 x_2 \\ &\quad - \frac{\bar{P}_{v,v,v}}{32}(v_0, T_0)(x_1^4 + x_2^4 + 4x_1^2 x_2^2) - \bar{P}_T(v_0, T_0)\epsilon\gamma \cos(\omega t)x_1 \\ &\quad - \bar{P}_{v,T}(v_0, T_0)\epsilon\gamma \cos(\omega t)x_1 x_2 - \frac{\bar{P}_{v,v,T}}{24}(v_0, T_0)3\epsilon\gamma \cos(\omega t)x_1(x_1^2 + 2x_2^2) \\ &\quad + \frac{Aq^2}{2}(x_1^2 + 4x_2^2). \end{aligned} \quad (3.5)$$

Let us note that the above form of the Hamiltonian is quite generic and is valid for any black hole in extended phase space thermodynamics. For the particular case of charged GB black holes, the relevant Hamiltonian is found to be:

$$\begin{aligned} H(x, u) &= \frac{u_1^2 + u_2^2}{2} + \frac{Aq^2}{2}(x_1^2 + 4x_2^2) - \frac{9\pi^2}{128}\epsilon\gamma \cos(\omega t)(32k\alpha + 9v_0^2)x_1 - \frac{81\pi^2}{128}\epsilon\gamma \cos(\omega t)v_0 x_1 x_2 \\ &\quad - \frac{1}{4} \left( \frac{81\pi^2 T_0}{64} + \frac{16\pi Q^2}{3v_0^5} \right) x_1^2 x_2 - \frac{1}{2} \left( -\frac{4\pi Q^2}{3v_0^4} + \frac{9\pi}{128}(-6k + 18\pi T_0 v_0) \right) (x_1^2 + x_2^2) \\ &\quad - \frac{81\pi^2}{512}\epsilon\gamma \cos(\omega t)x_1(x_1 + 2x_2^2) + \frac{5\pi Q^2}{6v_0^6}(x_1^4 + x_2^4 + 4x_1^2 x_2^2). \end{aligned} \quad (3.6)$$

Here,  $(x_1, x_2)$  and  $(u_1, u_2)$  are position and velocities of first two modes, and the corresponding equation of motion are:

$$\begin{aligned} \dot{x}_1 &= \frac{\partial H_2}{\partial u_1} = u_1, \\ \dot{x}_2 &= \frac{\partial H_2}{\partial u_2} = u_2, \end{aligned} \quad (3.7)$$

$$\begin{aligned}
\dot{u}_1 = & -\frac{\partial H_2}{\partial x_1} - \epsilon\mu_0qu_1 = \frac{9\pi^2}{128}\epsilon\gamma\cos(\omega t)(32k\alpha + 9v_0^2) - Aq^2x_1 \\
& + \left(-\frac{4\pi Q^2}{3v_0^4} + \frac{9\pi^2}{128}(-6k + 18T_0v_0)\right)x_1 + \frac{81\pi^2}{256}\epsilon\gamma\cos(\omega t)x_1^2 \\
& + \frac{81\pi^2}{128}\epsilon\gamma\cos(\omega t)v_0x_2 + \frac{1}{2}\left(\frac{81\pi^2T_0}{64} + \frac{16\pi Q^2}{3v_0^5}\right)x_1x_2 + \frac{81\pi^2}{512}\epsilon\gamma\cos(\omega t)(x_1^2 + 2x_2^2) \\
& - \frac{5\pi Q^2}{6v_0^6}(4x_1^3 + 8x_1x_2^2) - q\epsilon\mu_0u_1,
\end{aligned} \tag{3.8}$$

$$\begin{aligned}
\dot{u}_2 = & -\frac{\partial H_2}{\partial x_2} - 4\epsilon\mu_0qu_2 = +\frac{81}{128}\pi^2\epsilon\gamma\cos(\omega t)v_0x_1 + \frac{1}{4}\left(\frac{81\pi^2T_0}{64} + \frac{16\pi Q^2}{3v_0^5}\right)x_1^2 - 4Aq^2x_2 \\
& + \left(-\frac{4\pi Q^2}{3v_0^4} + \frac{9\pi^2}{128}(-6k + 18T_0v_0)\right)x_2 + \frac{81\pi^2}{128}\epsilon\gamma\cos(\omega t)x_1x_2 \\
& - \frac{5\pi Q^2}{6v_0^6}(4x_2^3 + 8x_1^2x_2) - 4q\epsilon\mu_0u_2.
\end{aligned} \tag{3.9}$$

Writing  $z = (x_1, x_2, u_1, u_2)^T$ , eqns. (3.7)-(3.9) can be written in a compact form as  $\dot{z}(t) = f_0(z) + \epsilon f_1(z, t)$ ;  $f_1$  is periodic in  $t$ , and the unperturbed system with  $\epsilon = 0$  is given as  $\dot{z}(t) = f_0(z)$ . If we linearize the unperturbed system about  $z = 0$ , we get  $\dot{z}_L(t) = Lz_L(t)$ . The matrix  $L$  can be computed to be [38, 43]:

$$\mathbf{L} = \begin{pmatrix} 0 & 0 & 1 & 0 \\ 0 & 0 & 0 & 1 \\ -Aq^2 + \psi & 0 & -\epsilon\mu_0q & 0 \\ 0 & -4Aq^2 + \psi & 0 & -4\epsilon\mu_0q \end{pmatrix}, \tag{3.10}$$

with eigen values:

$$\begin{aligned}
\lambda_{1,2} &= \frac{-\epsilon\mu_0q}{2} \pm \frac{1}{2}[\epsilon^2\mu_0^2q^2 - 4(Aq^2 - \psi)]^{\frac{1}{2}}, \\
\lambda_{3,4} &= -\frac{4\epsilon\mu_0q}{2} \pm [4\epsilon^2\mu_0^2q^2 - (4Aq^2 - \psi)]^{\frac{1}{2}}.
\end{aligned}$$

Here,

$$\psi = -\frac{4\pi Q^2}{3v_0^4} + \frac{9\pi}{128}(-6k + 18\pi T_0v_0).$$

Stability of the nodes depends on  $q^2$ . For  $q^2 < \frac{\psi}{A}$ , one notes that  $\lambda_1 > 0$ ,  $\lambda_2 < 0$  and both are real; while for  $q^2 > \frac{\psi}{4A}$ , both the eigen values  $\lambda_{3,4} = -\frac{4\epsilon\mu_0q}{2} \pm \iota[(4Aq^2 - (\psi))]^{\frac{1}{2}}$  are imaginary. Regarding  $\lambda_{1,2}$ , at least one of them has a positive real part and the other a negative real part, which signals a saddle point and an unstable equilibrium of the first node. On the other hand, both  $\lambda_{3,4}$  have a negative real part, indicating the existence of a spiral and a stable equilibrium of second and higher modes[43]. The solution of unperturbed system [39, 43], which is known to exist in the present case for the Hamiltonian given in eqn.(3.6) is:

$$z_0(t) = \begin{pmatrix} C_1 \operatorname{sech}(at) \\ 0 \\ C_2 \operatorname{sech}(at) \tanh(at) \\ 0 \end{pmatrix}, \tag{3.11}$$

where

$$a = (\psi - Aq^2)^{\frac{1}{2}}, \quad C_1 = \frac{av_0^3}{2Q} \sqrt{\frac{3}{5\pi}} \quad \text{and} \quad C_2 = -aC_1. \quad (3.12)$$

Having established the presence of a homoclinic orbit in eqn. (3.11) connecting the origin to itself in the unperturbed system, we now add the small temporal perturbation, and compute the Melnikov function defined earlier in eqn. (2.2) to be:

$$M(t_0) = - \int_{-\infty}^{+\infty} \left[ A_1 \gamma \cos(\omega t) \chi \xi + A_2 \gamma \cos(\omega t) \xi^3 \chi - q\mu_0 A_3 \xi^2 \chi^2 \right], \quad (3.13)$$

where  $\chi = \text{sech}(a(t - t_0))$  and  $\xi = \tanh(a(t - t_0))$ . Further,  $A_1 = (\frac{9\pi^2 k\alpha}{4} + \frac{81\pi^2 v_0^2}{128})C_2$ ,  $A_2 = \frac{243\pi^2 C_2 C_1^2}{512}$  and  $A_3 = C_2^2$ . The evaluation of  $M(t_0)$  is best done using the residue theorem, resulting in:

$$M(t_0) = \mathbf{N}\gamma\omega \sin(\omega t_0) - q\mu_0 \mathbf{I}, \quad (3.14)$$

where

$$\mathbf{N} = A_4 \pi \text{sech}\left(\frac{\pi\omega}{2a}\right) \quad \text{and} \quad \mathbf{I} = \frac{\pi A_3}{2a}, \quad (3.15)$$

with

$$A_4 = \frac{C_2(\frac{81}{128}\pi^2 v_0^2 + \frac{9}{4}\pi^2 k\alpha)}{a^2} + \frac{C_1^2 C_2(\omega^2 + a^2)}{16a^4} \frac{81\pi^2}{64}, \quad \text{and} \quad A_3 = C_2^2. \quad (3.16)$$

$M(t_0)$  has simple zeros at  $\mathbf{N}\gamma\omega \sin(\omega t_0) - q\mu_0 \mathbf{I} = 0$ , giving the bound

$$\left| \frac{q\mu_0 \mathbf{I}}{\mathbf{N}\gamma\omega} \right| \leq 1. \quad (3.17)$$

Further, eqn.(3.17) translates in to a critical value for the perturbation parameter  $\gamma$  of eqn. (3.1), as follows:

$$\gamma_{\text{critical}} = \left( \frac{\sqrt{3512} a^5 v_0^3 q \cosh\left(\frac{\pi\omega}{2a}\right) C_1 \mu_0}{18\sqrt{5} Q \pi^{3/2} \omega (256a^2 k\alpha + 9a^2 C_1^2 + 9\omega^2 C_1^2 + 72a^2 v_0^2)} \right). \quad (3.18)$$

One notes from eqn. (3.18) that, a small perturbation with  $\gamma > \gamma_{\text{critical}}$  guarantees the transversal intersection of stable and unstable manifolds, including the possible occurrence of Smale horseshoe chaotic motion [41, 46]. Chaotic behavior can be noted from figure-(4), where a numerical plot of time evolution of equations of motion in (3.7)-(3.9) is presented (for simplicity,  $x_2, u_2$  are set to zero). Plots in figure-(4)(a) and figure-(4)(b) show normal trajectories of the system, in the absence and presence of a small perturbation (but, for  $\gamma < \gamma_{\text{critical}}$ ), respectively. Figure-(4)(c) shows the onset of chaotic trajectories for  $\gamma > \gamma_{\text{critical}}$ . The value of  $\gamma$  that needs to be chosen for chaotic behavior is shown as the shaded region in the figures-(5)(a) and (5)(b), which essentially correspond to the plots of eqn. (3.18). Wherever not mentioned, all the parameters are taken to be unity and with out loss of generality, specific values of  $\alpha$  and/or  $Q$  etc., need to be chosen for obtaining the plots. In any case, the plots in figures-(5)(a) and (5)(b) are only suggestive and the actual expression of bound for  $\gamma$  given in eqn. (3.18) is to be used for actual computation of the allowed range. It is interesting to note from eqn. (3.11),

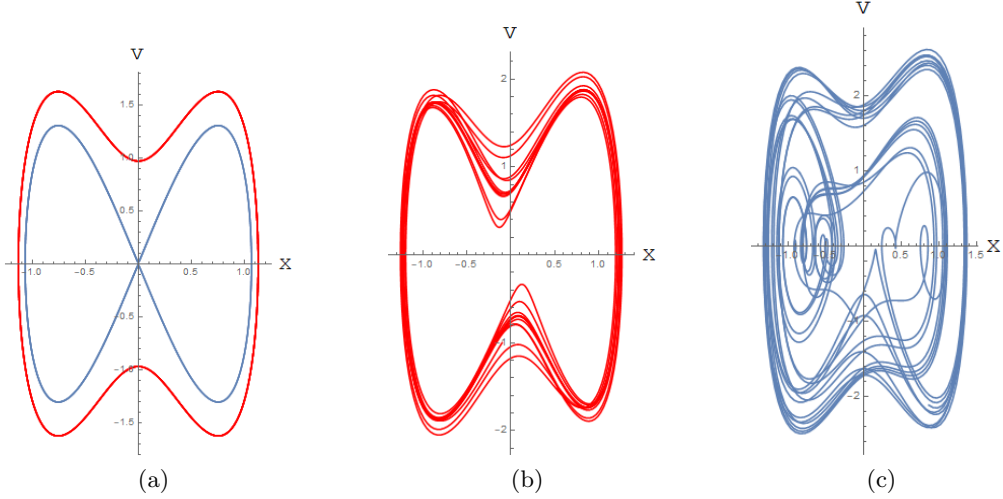


Figure 4: Plots show time evolution in the phase space of velocity vs displacement for (a)  $\epsilon = 0$  (b)  $\epsilon \neq 0, \gamma < \gamma_{\text{critical}}$  (c)  $\epsilon \neq 0, \gamma > \gamma_{\text{critical}}$

that the homoclinic orbit does not exist for  $Q = 0$ , as the non-linear term leading to such an orbit, is absent from the Hamiltonian in eqn. (3.6). The non-linear term in the Hamiltonian in eqn.(3.6) can be traced back to the  $\bar{P}_{v,v,v}(v_0, T_0)$  term in eqn.(3.5). As seen from eqn. (3.4), this term vanishes for  $Q = 0$ . Thus, we conclude that for neutral Gauss-Bonnet black holes, chaos under temporal perturbations does not occur, unless the black hole carries charge. Noting the importance of the non-vanishing nature of  $\bar{P}_{v,v,v}(v_0, T_0)$ , the above results can be generalized to more general black hole systems, by asking: what is the minimum power of  $v$ , that needs to be present in the equation of state for nonlinearity to appear in the Hamiltonian and lead to chaos? To answer this, let us assume a relation such as  $P \propto 1/v^n$ , for a generic black hole in extended phase thermodynamics, where  $n$  is the largest power of  $v$  that occurs in a given black hole equation of state<sup>2</sup> in a general dimension  $d$ . The condition to rule out non-linearity in the Hamiltonian in eqn.(3.5) and absence of chaotic behavior is that  $\bar{P}_{v,v,v}(v_0, T_0) = 0$ . Solving this equation, we get a relation between  $n$  and  $d$  as:

$$d = 2, n > 0, \quad d > i, n = d - i \quad \text{for } i = 3, 4, 5. \quad (3.19)$$

Let us note that the conditions in eqn. (3.19) are obtained for any generic black hole in AdS with extended phase thermodynamic description and can be used to rule out chaos based on the equation of state itself. For instance, as seen from eqn.(2.7), the largest power of  $v$  in the equation of state for a neutral Gauss-Bonnet black hole in a general dimension  $d$  is  $n = 4$ . Either one of the conditions, given in eqn. (3.19), is always satisfied for any  $d > 4$  for  $n = 4$ . We thus conclude that chaotic behavior under temporal perturbations would be absent for neutral Gauss-Bonnet black holes in any dimension. On the other hand, for charged GB black holes, there is a term in equation of state in eqn.(2.7), which contains higher powers of  $v$  and it can be checked that the conditions in eqn. (3.19) are not satisfied in any dimension. Thus, chaotic behavior is possible, once the perturbation parameters satisfy the constraints put forward in eqn. (3.18). These differences between neutral and charged black holes should be investigated

<sup>2</sup>This assumption is valid for most of the static black holes as the equation of state contains polynomials of  $v$ .

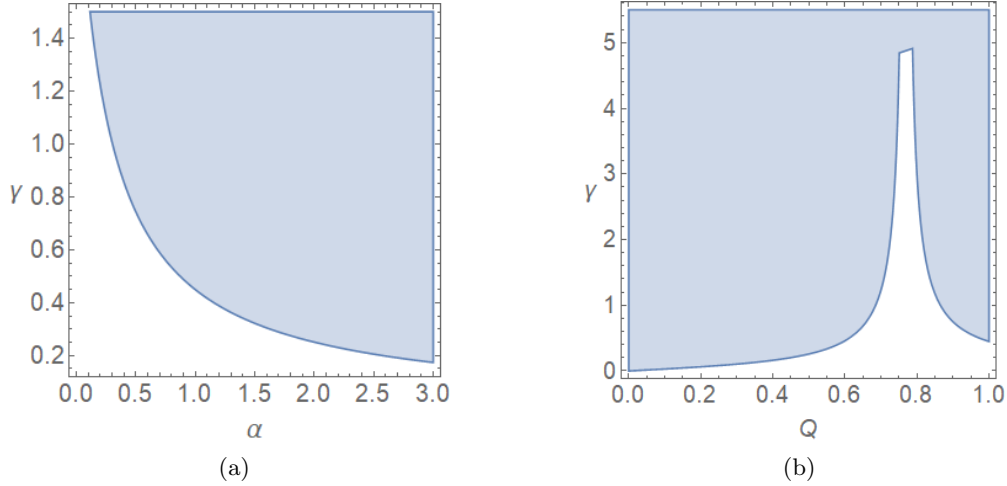


Figure 5: Shaded region denotes onset of chaotic motion:  $v_0 = 2.75, T_0 = 0.01$  (a)  $\gamma$  vs  $\alpha$  plot for charged GB black holes in  $d = 5$ , for  $Q = 1$  (b)  $\gamma$  vs  $Q$  plot for charged GB black holes in  $d = 5$  for  $\alpha = 1$

further for better understanding, especially, because the spinodal region in the PV diagram continues to exist, irrespective of the presence of charge  $Q$  or not. It is also important to note that many of above results depend crucially on the distinction made between thermodynamic volume  $V$  and specific volume  $v$  through the new effective equation of state in eqn. (3.4), while performing computations.

We now extend the results obtained above to more general case of Lovelock black holes in higher dimensions and check for chaotic behavior. The details of the action and PV critical behavior

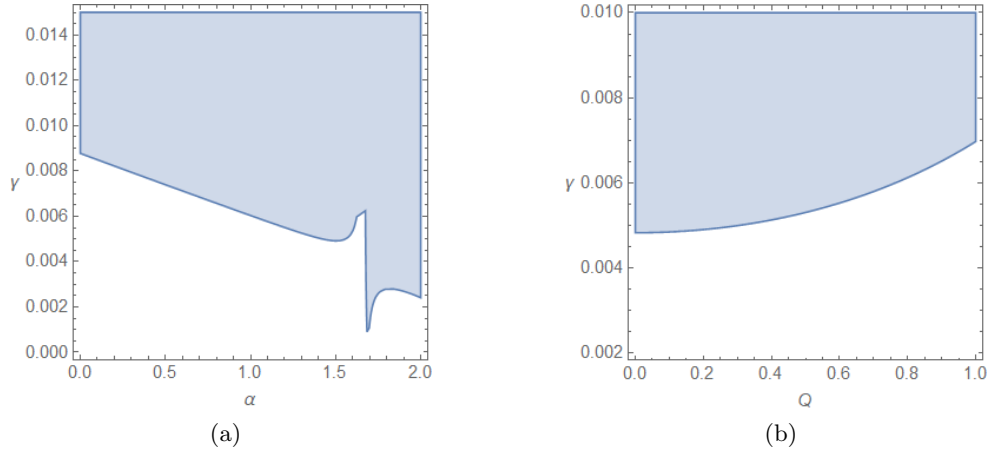


Figure 6: Charged Lovelock Black holes in  $d = 7$ , with  $v_0 = 1.44, T_0 = 0.1$ : Plots of (a)  $\gamma$  vs  $\alpha$  for  $Q = 2$  and (b)  $\gamma$  vs  $Q$  for  $\alpha = 1$ . Values of  $\gamma$  in the shaded region lead to onset of chaotic motion

are discussed in detail in [65, 66] and we only need to recall the equation of state given as:

$$P = \frac{T}{v} + \frac{32k\alpha T}{(d-2)^2 v^3} + \frac{256k^2 T \alpha^2}{(d-2)^4 v^5} - \frac{(d-3)k}{(d-2)\pi v^2} - \frac{16k^2(d-5)\alpha}{(d-2)^3 \pi v^4} - \frac{256k^3(d-7)\alpha^2}{3(d-2)^5 \pi v^6} + \frac{16^{d-3}(d-3)Q^2}{\pi(d-2)^{(2d-5)}v^{(2d-4)}}. \quad (3.20)$$

It is known that a Van der Waals type phase transition exists in these theories, together with a presence of spinodal unstable region. The procedure discussed in this section can be straightforwardly extended to the present case in all dimensions, starting from the equation of state in eqn.(3.20) in general dimensions. Applying the condition in eqn. (3.19) to the equation of state in eqn. (3.20) above, chaos can be ruled out for neutral third order Lovelock black holes starting from dimension  $d = 7$ . For the charged case, however, the nonlinear terms following from the relevant Hamiltonian in eqn. (3.5) will be present and we see below that chaotic behaviour above a certain value of  $\gamma$  persists. We have computed analytically the expressions for Hamiltonian, Melnikov functions and associated bound on  $\gamma$ , but they are cumbersome and otherwise not very illuminating. We suppress the expressions and present a plot of  $\gamma$  vs  $\alpha$  and  $Q$  in seven dimensions in figure-(6), where the shaded parts show the allowed regions of  $\gamma$  for which temporal chaos will be present. It is also useful to mention that the plots in figure-(6) are only suggestive and are obtained after choosing specific values of parameters being varied. For knowing the actual bound, the exact analytical expressions are to be used.

Now, let us comment on the chaotic behaviour in the case of RN AdS black holes in general dimensions. In this case, the equation of state is given as [69]:

$$P = \frac{T}{v} - \frac{d-3}{(d-2)\pi v^2} + \frac{(d-3)2^{4(d-3)}Q^2}{(d-2)^{2d-5}\pi v^{2(d-2)}}. \quad (3.21)$$

It can be checked explicitly, that none of the conditions in eqn. (3.19) are satisfied in any dimension and hence chaos will exist beyond a certain value of the perturbation parameter  $\gamma$  in RN AdS black holes in any dimension. As the Gauss-Bonnet terms are total derivative terms in four dimensions, we can start comparing with the RN AdS case (by setting  $\alpha = 0$ ), starting from five dimensions. In fact, setting  $\alpha = 0$  in eqn. (3.18), gives the limit on  $\gamma$ , beyond which chaos will exist in RN AdS black holes in five dimensions. The corresponding result in four dimensions was explicitly computed in [38]. Thus, the conclusion that chaotic behaviour should be present in the four dimensional example of RN AdS black holes, studied in [38], is in conformity with our general condition in eqn. (3.19). Furthermore, as  $\alpha$  increases, it can be noted from figure-5(a), that the GB system becomes chaotic for even smaller values of the perturbation parameter  $\gamma$ .

To conclude this section, we note that the presence of charge  $Q$  is necessary for triggering chaos under temporal perturbations in the extended thermodynamic phase space of black hole systems.

## 4 Spatial Perturbations and Chaos

In this section, our aim is to study the effect of a small spatially periodic perturbation in the equilibrium state solutions about a sub-critical temperature given as follows [43]:

$$T = T_0 + \epsilon \cos(qx). \quad (4.1)$$

Korteweg's theory gives the Piola stress tensor as [43]:

$$\tau = -P(v, T) - Av'' \quad (4.2)$$

where  $'$  stands for  $\frac{d}{dx}$ .  $P(v, T)$  is supplied by the GB black hole equation of state from eqn.(2.11) and  $T$  is absolute temperature with  $A > 0$ . For zero body force balance of linear momentum, one sets  $\tau' = 0$ , giving  $\tau = B = \text{constant}$ . Thus,  $B$  is the ambient pressure as  $|x| \rightarrow \infty$ ; using this, eqn.(4.2) yields:

$$v'' + P(v, T) = B. \quad (4.3)$$

Let us start by discussing the unperturbed system, where one starts by setting  $T = T_0$  in eqn.(4.3). The fixed points of the system in eqn.(4.3) can be found, which are the specific volume corresponding to ambient pressure  $B$  for different given temperatures. We choose a set of sample temperatures,  $0.8T_c$  and  $0.7T_c$  and call the corresponding fixed points as  $(v_1, v_2, v_3)$  and  $(w_1, w_2, w_3)$ . For the case of  $T_0 = 0.8T_c$ , these are shown in figure 7, with analogous construction assumed at  $T_0 = 0.7T_c$ . Let us note that Maxwell equal Area construction for

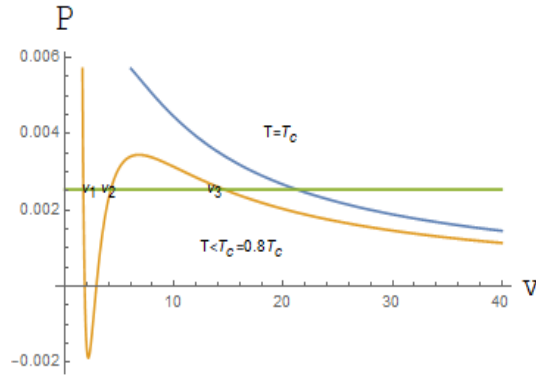


Figure 7: Charged GB Maxwell Equal Area construction for  $Q=1$ ,  $\alpha = 1$ ,  $k=1$ ,  $T = 0.8T_c$

Gauss Bonnet black holes done in [64] is useful while plotting figure-7. Now, from eqn.(4.3) and figure-7, one infers three different kinds of orbits in  $v' - v$  phase plane.

- Case-1: In this case we choose the pressure in the range  $P(v_1, T_0) < B < P(v_2, T_0)$  and get a homoclinic orbit connecting a saddle point  $v_3$  to itself. Corresponding phase orbits are shown in figures-8(a) and 8(b) for charged and neutral black holes, respectively.
- Case-2: Choosing the pressure in the range  $P(v_1, T_0) < B < P(v_2, T_0)$ , results in a homoclinic orbit connecting a saddle point  $v_1$  to itself, as in case-1 above. Corresponding phase orbits are presented in figures-9(a) and 9(b) for charged and neutral black holes, respectively.
- Case-3: In this case the pressure is taken such that,  $P(v_1, T_0) = B = P(v_2, T_0)$ ; This results in a heteroclinic orbit connecting  $v_1$  with  $v_3$ . Corresponding phase orbits are shown in figures-10(a) and 10(b) for charged and neutral black holes, respectively.

Including a small spatial perturbation given in eqn.(4.1), we can rewrite the eqn.(4.3) for perturbed system as follows:

$$v'' = B - P(v, T_0) - \frac{\epsilon \cos(qx)}{v} \quad (4.4)$$

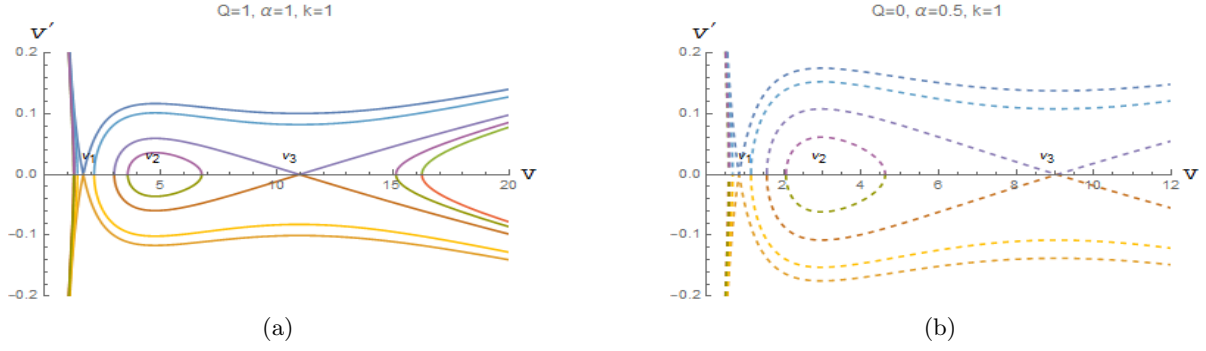


Figure 8: Case1: (a) Charged Gauss-Bonnet with  $v_1 = 1.68107, v_2 = 4.77519, v_3 = 10.9746$ . (b) Neutral Gauss-Bonnet with  $v_1 = 0.849379, v_2 = 2.97856, v_3 = 9.04772$

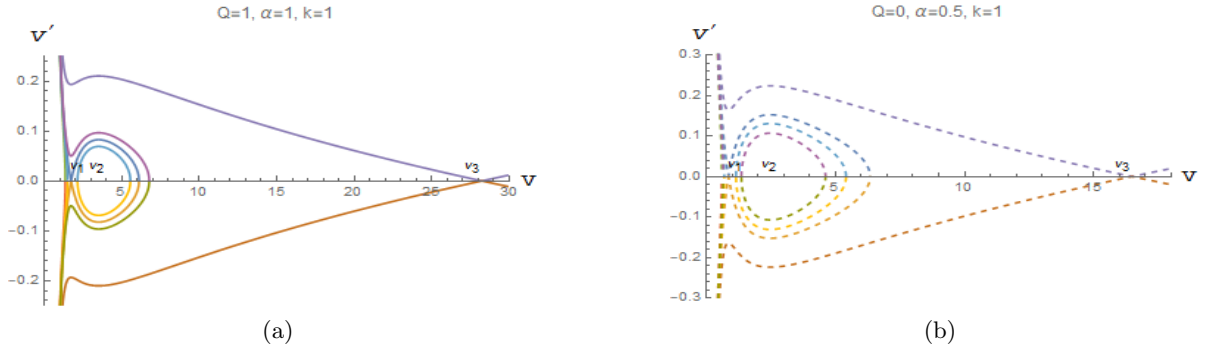


Figure 9: Case2: (a) Charged Gauss-Bonnet with  $v_1 = 1.73389, v_2 = 3.51509, v_3 = 28.2263$ . (b) Neutral Gauss-Bonnet with  $v_1 = 0.862346, v_2 = 2.47978, v_3 = 16.4746$ .

Melnikov function from eqn. (2.2) written suitably for spatially perturbed systems is:

$$M(x_0) = \int_{-\infty}^{\infty} f(z(x-x_0))\Omega_{n=1}g(z(x-x_0), x)dx \quad (4.5)$$

Setting  $v' = h$ , eqn.(4.4) converts to a set of first order equations as:

$$\begin{aligned} v' &= h \\ h' &= B - P(v, T_0) - \frac{\epsilon \cos(qx)}{v} \end{aligned} \quad (4.6)$$

As in the previous section, writing general solutions for (homoclinic or heteroclinic) orbit as:

$$z(x) = \begin{pmatrix} v_0(x-x_0) \\ h_0(x-x_0) \end{pmatrix}, \quad (4.7)$$

and using them in eqn.(4.4), one can write  $f(z(x-X_0))$  and  $g(z(x-x_0), x)$  as

$$f(z(x-X_0)) = \begin{pmatrix} h_0(x-x_0) \\ B - P(v_0(x-x_0), T_0) \end{pmatrix}, \quad g(z(x-X_0), x) = \begin{pmatrix} 0 \\ -\frac{\cos(qx)}{v_0(x-x_0)} \end{pmatrix}. \quad (4.8)$$

Using these in eqn.(4.5), Melnikov function is finally:

$$M(x_0) = - \int_{-\infty}^{+\infty} \frac{h_0(x-x_0) \cos(qx)}{v_0(x-x_0)} dx$$

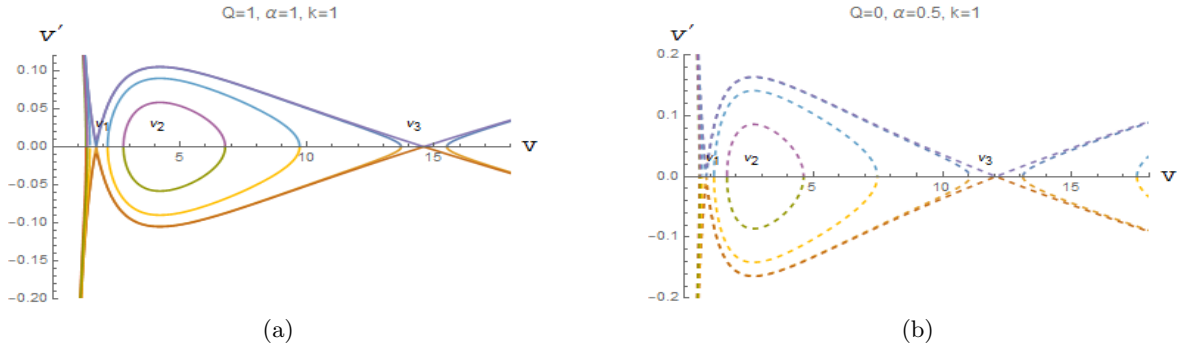


Figure 10: Case3: (a) Charged Gauss-Bonnet with  $v_1 = 1.69635, v_2 = 4.20704, v_3 = 14.593$ . (b) Neutral Gauss-Bonnet with  $v_1 = 0.855689, v_2 = 2.68773, v_3 = 12.0659$ .

Changing variables to  $R = x - x_0$ , the Melnikov function becomes:

$$M(x_0) = -L \cos(qx_0) + W \sin(qx_0)$$

with

$$L = \int_{-\infty}^{\infty} \frac{h_0(R) \cos(qR)}{v_0(R)} dR, \quad W = \int_{-\infty}^{\infty} \frac{h_0(R) \sin(qR)}{v_0(R)} dR. \quad (4.9)$$

From the structure of Melnikov function and following the arguments in [43],  $M(x_0)$  always possesses simple zeros, signalling chaos. The results of this section can be carried over to charged Lovelock black holes in various dimensions and we have checked that the general features found in this section continue to exist, namely the system exhibits homoclinic orbits for the cases-1 and 2 discussed above; For case-3, the system has homoclinic as well as heteroclinic orbits. The presence of chaos under spatial perturbations is found in all three cases in Lovelock black holes in higher dimensions, irrespective of whether the charge is present or not, unlike the case of temporal perturbations discussed in last section.

## 5 Conclusions

In this work, we studied the emergence of chaotic behaviour under temporal and spatial perturbations in the spinodal region of charged and neutral Gauss-Bonnet black holes in extended thermodynamic phase space. The perturbed Hamiltonian system corresponding to the motion of the fluid in the spinodal region, following from the black hole equation of state was obtained and shown to possess nonlinear terms giving homoclinic/heteroclinic orbits in phase space. Analysis of the zeroes of the appropriate Melnikov functions gives information about the onset of chaos in the thermodynamic phase space. As regards temporal perturbations, chaotic behaviour is found to be present in charged GB black holes in five dimensions. The zeros of the Melnikov function give a bound on the perturbation parameter for chaos to exist. This was computed analytically, such as the one in eqn.(3.18) and depends on the charge  $Q$  and the GB coupling  $\alpha$ . It is important to note that in this paper, the computations were performed explicitly in five dimensions, as the Gauss-Bonnet term is a total derivative in four dimensions and does not effect the black hole solution. Setting the GB coupling  $\alpha = 0$  in eqn. (3.18),

gives us the bound on  $\gamma$  for chaos to exist, for the corresponding RN AdS black holes in five dimensions. These general conclusions hold true in any dimension, based on the condition in eqn. (3.19). For instance, based on eqns. (3.19) and (3.21), it can be said that in four dimensions, chaotic behaviour should exist beyond a certain value of  $\gamma$ . This result is in conformity with the analysis in [38] where the explicit value of  $\gamma$  was computed in four dimensions. When  $\alpha$  is non-zero, we find that the onset of chaotic behaviour occurs for even lower values of the temporal perturbation parameter  $\gamma$ , showing the sensitivity of chaotic behaviour in the presence of GB terms. Intriguingly, the chaotic behaviour under temporal perturbations is not present for neutral GB and Lovelock black holes in general dimensions, which needs to be investigated further. A general condition was derived in eqn.(3.19), which can be used to rule out chaos under temporal perturbations in general dimensions by analysing the equation of state provided by the black hole. In every dimension, for chaos to exist, the highest power of  $v$  in the equation of state, cannot be lower than a certain value (as governed by eqn. (3.19)). The reason for existence of chaotic behaviour in charged black holes is that the term dependent on charge  $Q$  in the black hole equation of state, increases quadratically with  $v$ , as the number of dimensions increases. This can be seen from the last term in the GB and RN AdS equations of state given in eqn. (2.7) and (3.21), respectively. Thus, chaotic behaviour crucially depends on the number of dimensions as well as the equation of state of the black hole. It is also important to mention that many of above results depend crucially on the distinction made between thermodynamic volume  $V$  and specific volume  $v$ . In particular, we expressed the pressure  $P$  in terms of the specific volume  $v$ , through the new effective equation of state in eqn. (3.4), while performing computations. The use of effective equation of state in eqn. (3.4) is important in concluding the existence or non-existence of chaos

Under spatial perturbations, existence of homoclinic and heteroclinic orbits is found to exist in charged as well as neutral GB black holes and the phase space plots were given. The extension of results to Lovelock black holes in higher dimensions was discussed. It would be interesting to understand the holographic aspects of these chaotic behaviour, particularly found in the unstable small/large black hole phase transition domain, not just in GB black holes, but also in other charged and neutral black holes in AdS, considering other stringy corrections. More importantly, the absence of chaos in neutral black holes needs to be understood better.

## Acknowledgements

The authors would like to thank the anonymous referee for helpful suggestions.

## References

- [1] Jacob D. Bekenstein. Black holes and entropy. *Phys. Rev. D*, 7:2333–2346, Apr 1973.
- [2] Jacob D. Bekenstein. Generalized second law of thermodynamics in black-hole physics. *Phys. Rev. D*, 9:3292–3300, Jun 1974.
- [3] S. W. Hawking, “Particle Creation by Black Holes,” *Commun. Math. Phys.* **43**, 199 (1975) Erratum: [*Commun. Math. Phys.* **46**, 206 (1976)].

- [4] S. W. Hawking, “Black Holes and Thermodynamics,” *Phys. Rev. D* **13**, 191 (1976).
- [5] G. W. Gibbons and S. W. Hawking, “Action Integrals and Partition Functions in Quantum Gravity,” *Phys. Rev. D* **15**, 2752 (1977).
- [6] S. W. Hawking and D. N. Page, “Thermodynamics of Black Holes in anti-De Sitter Space,” *Commun. Math. Phys.* **87**, 577 (1983).
- [7] J. M. Maldacena, “The Large N limit of superconformal field theories and supergravity,” *Int. J. Theor. Phys.* **38**, 1113 (1999) [*Adv. Theor. Math. Phys.* **2**, 231 (1998)] [[hep-th/9711200](#)].
- [8] E. Witten, “Anti-de Sitter space and holography,” *Adv. Theor. Math. Phys.* **2**, 253 (1998) [[hep-th/9802150](#)].
- [9] S. S. Gubser, I. R. Klebanov and A. M. Polyakov, “Gauge theory correlators from noncritical string theory,” *Phys. Lett. B* **428**, 105 (1998) [[hep-th/9802109](#)].
- [10] D. Kastor, S. Ray, and J. Traschen, “Enthalpy and the Mechanics of AdS Black Holes,” *Class.Quant.Grav.* **26** (2009) 195011, [[arXiv:0904.2765](#) [[hep-th](#)]].
- [11] M. M. Caldarelli, G. Cognola, and D. Klemm, “Thermodynamics of Kerr-Newman-AdS black holes and conformal field theories,” *Class.Quant.Grav.* **17** (2000) 399–420, [[arXiv:hep-th/9908022](#) [[hep-th](#)]].
- [12] S. Wang, S.-Q. Wu, F. Xie, and L. Dan, “The First laws of thermodynamics of the (2+1)-dimensional BTZ black holes and Kerr-de Sitter spacetimes,” *Chin.Phys.Lett.* **23** (2006) 1096–1098, [[arXiv:hep-th/0601147](#) [[hep-th](#)]].
- [13] Y. Sekiwa, “Thermodynamics of de Sitter black holes: Thermal cosmological constant,” *Phys.Rev.* **D73** (2006) 084009, [[arXiv:hep-th/0602269](#) [[hep-th](#)]].
- [14] E. A. Larranaga Rubio, “Stringy Generalization of the First Law of Thermodynamics for Rotating BTZ Black Hole with a Cosmological Constant as State Parameter,” [[arXiv:0711.0012](#) [[gr-qc](#)]].
- [15] B. P. Dolan, “The cosmological constant and the black hole equation of state,” *Class.Quant.Grav.* **28** (2011) 125020, [[arXiv:1008.5023](#) [[gr-qc](#)]].
- [16] M. Cvetič, G. Gibbons, D. Kubiznak, and C. Pope, “Black Hole Enthalpy and an Entropy Inequality for the Thermodynamic Volume,” *Phys.Rev.* **D84** (2011) 024037, [[arXiv:1012.2888](#) [[hep-th](#)]].
- [17] B. P. Dolan, “Pressure and volume in the first law of black hole thermodynamics,” *Class.Quant.Grav.* **28** (2011) 235017, [[arXiv:1106.6260](#) [[gr-qc](#)]].
- [18] M. Henneaux and C. Teitelboim, “The Cosmological Constant as a Canonical Variable,” *Phys.Lett.* **B143** (1984) 415–420.
- [19] C. Teitelboim, “The Cosmological Constant as a Thermodynamic Black Hole Parameter,” *Phys.Lett.* **B158** (1985) 293–297.

- [20] M. Henneaux and C. Teitelboim, “The Cosmological Constant and General Covariance,” *Phys.Lett.* **B222** (1989) 195–199.
- [21] C. V. Johnson and F. Rosso, “Holographic Heat Engines, Entanglement Entropy, and Renormalization Group Flow,” *Class. Quant. Grav.* **36**, no. 1, 015019 (2019) [arXiv:1806.05170 [hep-th]].
- [22] A. Chamblin, R. Emparan, C. V. Johnson, and R. C. Myers, *Phys. Rev. D* **60**, 064018 (1999); *ibid.* **60** 104026 (1999).
- [23] A. Chamblin, R. Emparan, C. V. Johnson and R. C. Myers, “Holography, thermodynamics and fluctuations of charged AdS black holes,” *Phys. Rev. D* **60**, 104026 (1999) [hep-th/9904197].
- [24] D. Kubiznak, R. B. Maan, *JHEP* **1207**, 033 (2012).
- [25] D. Kubiznak, R. B. Mann and M. Teo, “Black hole chemistry: thermodynamics with Lambda,” *Class. Quant. Grav.* **34**, no. 6, 063001 (2017) [arXiv:1608.06147 [hep-th]].  
[26]
- [26] S. Gunasekaran, R. B. Mann and D. Kubiznak, “Extended phase space thermodynamics for charged and rotating black holes and Born-Infeld vacuum polarization,” *JHEP* **1211**, 110 (2012) [arXiv:1208.6251 [hep-th]].
- [27] L. Bombellitf and E. Calzetta, Chaos around a black hole, *Class. Quant. Grav.* **9** (1992) 2573 .
- [28] P. S. Letelier and W. M. Vieira, “Chaos in black holes surrounded by gravitational waves,” *Class. Quant. Grav.* **14** (1997) 1249.
- [29] M. Santoprete and G. Cicogna, “Chaos in black holes surrounded by electromagnetic fields,” *Gen. Rel. Grav.* **34** (2002) 1107.
- [30] G. A. Monerat, H. P. de Oliveira and I. D. Soares, “Chaos in preinflationary Friedmann-Robertson-Walker universes,” *Phys. Rev. D* **58** (1998) 063504 .
- [31] G. N. Felder and L. Kofman, “Nonlinear inflaton fragmentation after preheating,” *Phys. Rev. D* **75** (2007) 043518 .
- [32] F. L. Dubeibe, L. A. Pachon and J. D. Sanabria-Gomez, “Chaotic dynamics around astrophysical objects with nonisotropic stresses,” *Phys. Rev. D* **75** (2007) 023008.
- [33] J. R. Gair, C. Li and I. Mandel, “Observable Properties of Orbits in Exact Bumpy Spacetimes,” *Phys. Rev. D* **77** (2008) 024035.
- [34] S. Chen, M. Wang and J. Jing, “Chaotic motion of particles in the accelerating and rotating black holes spacetime,” *JHEP* **1609** (2016) 082.
- [35] V. Cardoso, A. S. Miranda, E. Berti, H. Witek and V. T. Zanchin, “Geodesic stability, Lyapunov exponents and quasinormal modes,” *Phys. Rev. D* **79**, 064016 (2009) [arXiv:0812.1806 [hep-th]].

- [36] R. A. Konoplya and Z. Stuchlík, “Are eikonal quasinormal modes linked to the unstable circular null geodesics?,” *Phys. Lett. B* **771**, 597 (2017) [arXiv:1705.05928 [gr-qc]].
- [37] V. K. Melnikov, *Trans. Moscow Math. Soc.* **12** (1963) 1; J. Guckenheimer and P. J Holmes, *Nonlinear Oscillations, Dynamical Systems, and Bifurcations of Vector Fields*, Applied Math. Sciences. Vol. **42** (1983), Springer-Verlag, New York.
- [38] M. Chabab, H. El Moumni, S. Iraoui, K. Masmar and S. Zhizeh, “Chaos in charged AdS black hole extended phase space,” *Phys. Lett. B* **781**, 316 (2018) [arXiv:1804.03960 [hep-th]].
- [39] P. Holmes, A nonlinear oscillator with a strange attractor, *Phil. Trans. Roy. Soc. A* **292** (1979) 419.
- [40] P. Holmes, A partial differential equation with infinitely many periodic orbits: Chaotic oscillations of a forced beam, *Archive for Rational Mechanics and Analysis*, **76**, 2 (1981) 135–165.
- [41] P. Holmes, Poincare celestial mechanics, dynamical-systems theory and chaos, *Phys. Rep.* **193** (1990) 137.
- [42] G. D. Birkhoff, *Nouvelles recherches sur les systemes dynamiques*, Collected Mathematical Papers, Vol. 2, Amer. Math. Soc, Providence, R . L, 1950,p p. 530-662.; S. Smale, Diffeomorphisms with many periodic points, *Differential and Combinatorial Topology*, Princeton Univ. Press, Princeton, N. J., 1965, pp. 63-80.
- [43] M. Slemrod, Temporal and Spatial Chaos in a van der Waals Fluid Due to Periodic Thermal Fluctuations, *Advances Applied Math.* **D 6** (1985) 135 .
- [44] B. U. Felderhof, Dynamics of the diffuse gas-liquid interface near the critical point, *Physica.* **D 48** (1970) 541.
- [45] B. Widom, Structure and thermodynamics of interfaces, in U. Landman (Ed.), *Statistical Mechanics and Statistical Methods in Theory and Application*, Plenum, New York, 1977.
- [46] S. Smale, Diffeomorphisms with many periodic points, *Matematika*, **11** (4) (1967) 88. ; *Differential and Combinatorial Topology (A Symposium in Honor of Marston Morse)*, (1965) 63-80.
- [47] D. Lovelock, “The Einstein tensor and its generalizations,” *J. Math. Phys.* **12**, 498 (1971).
- [48] B. Zwiebach, “Curvature Squared Terms and String Theories,” *Phys. Lett.* **156B**, 315 (1985).
- [49] D. G. Boulware and S. Deser, “String Generated Gravity Models,” *Phys. Rev. Lett.* **55**, 2656 (1985).
- [50] D. L. Wiltshire, “Spherically Symmetric Solutions of Einstein-maxwell Theory With a Gauss-Bonnet Term,” *Phys. Lett.* **169B**, 36 (1986).

- [51] R. C. Myers and J. Z. Simon, “Black Hole Thermodynamics in Lovelock Gravity,” *Phys. Rev. D* **38**, 2434 (1988).
- [52] D. L. Wiltshire, “Black Holes in String Generated Gravity Models,” *Phys. Rev. D* **38**, 2445 (1988).
- [53] S. Nojiri and S. D. Odintsov, “Anti-de Sitter black hole thermodynamics in higher derivative gravity and new confining deconfining phases in dual CFT,” *Phys. Lett. B* **521**, 87 (2001) Erratum: [*Phys. Lett. B* **542**, 301 (2002)] [hep-th/0109122].
- [54] R. G. Cai, “Gauss-Bonnet black holes in AdS spaces,” *Phys. Rev. D* **65**, 084014 (2002) [hep-th/0109133].
- [55] A. Sen, “Entropy function for heterotic black holes,” *JHEP* **0603**, 008 (2006) [hep-th/0508042].
- [56] M. Brigante, H. Liu, R. C. Myers, S. Shenker and S. Yaida, “Viscosity Bound Violation in Higher Derivative Gravity,” *Phys. Rev. D* **77**, 126006 (2008) [arXiv:0712.0805 [hep-th]].
- [57] R. G. Cai, Z. Y. Nie, N. Ohta and Y. W. Sun, “Shear Viscosity from Gauss-Bonnet Gravity with a Dilaton Coupling,” *Phys. Rev. D* **79**, 066004 (2009) [arXiv:0901.1421 [hep-th]].
- [58] C. V. Johnson, “Gauss–Bonnet black holes and holographic heat engines beyond large  $N$ ,” *Class. Quant. Grav.* **33**, no. 21, 215009 (2016) [arXiv:1511.08782 [hep-th]].
- [59] M. M. Qaemmaqami, “Criticality in third order lovelock gravity and butterfly effect,” *Eur. Phys. J. C* **78**, no. 1, 47 (2018) [arXiv:1705.05235 [hep-th]].
- [60] C. Bhamidipati and P. K. Yerra, “A note on Gauss–Bonnet black holes at criticality,” *Phys. Lett. B* **772**, 800 (2017) [arXiv:1706.09344 [hep-th]].
- [61] R. G. Cai, L. M. Cao, L. Li and R. Q. Yang, “P-V criticality in the extended phase space of Gauss-Bonnet black holes in AdS space,” *JHEP* **1309**, 005 (2013) [arXiv:1306.6233 [gr-qc]].
- [62] S. Q. Lan, J. X. Mo and W. B. Liu, “A note on Maxwell’s equal area law for black hole phase transition,” *Eur. Phys. J. C* **75**, no. 9, 419 (2015) [arXiv:1503.07658 [gr-qc]].
- [63] H. Xu and Z. M. Xu, “Maxwell’s equal area law for Lovelock thermodynamics,” *Int. J. Mod. Phys. D* **26**, no. 04, 1750037 (2016) [arXiv:1510.06557 [gr-qc]].
- [64] A. Belhaj, M. Chabab, H. El mounni, K. Masmar and M. B. Sedra, “Maxwell’s equal-area law for Gauss-Bonnet-Anti-de Sitter black holes,” *Eur. Phys. J. C* **75**, no. 2, 71 (2015) [arXiv:1412.2162 [hep-th]].
- [65] M. H. Dehghani, N. Alinejadi and S. H. Hendi, “Topological Black Holes in Lovelock-Born-Infeld Gravity,” *Phys. Rev. D* **77**, 104025 (2008) [arXiv:0802.2637 [hep-th]].
- [66] J. X. Mo and W. B. Liu, “ $P-V$  criticality of topological black holes in Lovelock-Born-Infeld gravity,” *Eur. Phys. J. C* **74**, no. 4, 2836 (2014) [arXiv:1401.0785 [gr-qc]].
- [67] E. J. Kim and S. Kawai, “Chaotic dynamics of the Bianchi IX universe in Gauss-Bonnet gravity,” *Phys. Rev. D* **87**, no. 8, 083517 (2013) [arXiv:1301.6853 [gr-qc]].

- [68] D. Z. Ma, J. P. Wu and J. Zhang, “Chaos from the ring string in a Gauss-Bonnet black hole in AdS5 space,” *Phys. Rev. D* **89**, no. 8, 086011 (2014) [arXiv:1405.3563 [hep-th]].
- [69] A. Belhaj, M. Chabab, H. El Moumni and M. B. Sedra, “On Thermodynamics of AdS Black Holes in Arbitrary Dimensions,” *Chin. Phys. Lett.* **29**, 100401 (2012) [arXiv:1210.4617 [hep-th]].